JOURNAL OF PETROLEUM GEOMECHANICS
(JPG)

4D geomechanical simulations for field development planning

Jörg V. Herwanger
MP-Geomechanics, jherwanger@mpgeomechanics.com

Received: 10 Dec 2019; Accepted: 25 Feb 2019
DOI: 10.22107/JPG.2019.88409

Keywords
Case study, numerical model, calibration, wellbore stability, inclined well, fault stability, hydraulic stimulation, fracture containment

Abstract

3D and 4D geomechanical can be time-consuming to build and calibrate. However, once such a model is built, it is relative straightforward to use this model for various field development and management applications. In so doing, the return on the initial investment of time and effort in the creation of a 4D geomechanical model can be substantial. I present a case study where a 4D geomechanical model of a deepwater turbidite field under water flood is used to:

- Assessment of wellbore stability for drilling inclined infill wells after a stuck pipe event
- Calculation of maximum allowable injection pressures during hydraulic stimulation to avoid out-of-zone growth of stimulated fractures, and
- evaluation of risk of fault re-activation during a range of production scenarios for pressure support in order to establish safe operational limits for pressure support.

Model building uses seismic inversion volumes to constrain a geological facies model, followed by upscaling to a reservoir simulation model and history matching. Similarly, a 3D geomechanical property model is built to the seafloor. The calibration of the pre-production stress state of the geomechanical model comprises of matching the results of 3D finite element stress field calculations to 1D wellbore models. The calibration uses a novel method of linking tectonic strain terms in poro-elastic equations in the 1D and 3D models. Production and injection processes are the computed using a fully coupled finite element based geomechanical flow simulator, solving multi-phase (black-oil) fluid flow and geomechanics equations simultaneously on the same computational mesh. The computational mesh is optimized for geomechanical predictions of wellbore and fault stability.

1. INTRODUCTION

Geomechanical models have many applications in field development planning and reservoir management. The aim of this paper is to demonstrate some of the many uses of geomechanical and flow simulation technology in drilling operations and determination of operational limits for oil-extraction and fluid injection. I will do this using a case study from a deepwater turbidite reservoir. The paper is organized in two sections. First, I present model building and calibration. Here special emphasis is placed on the uses of seismic interpretations and inversion models in 3D model building, the importance of calibration, and the influence of the 3D property model on the computed stress field. In a second section, I discuss the

applications of the 4D geomechanical model to a range of field development planning issues, including (i) wellbore stability assessment for drilling inclined infill wells, as well as the change in mudweight window over time for planned wells during injection and production from the field, (ii) calculation of maximum allowable injection pressures during hydraulic stimulation to avoid out-of-zone growth of hydraulic fractures, and (iii) evaluation of risk of fault re-activation during a range of production scenarios for pressure support in order to establish safe operational limits for pressure support.

During this study we noticed, maybe to our surprise, that additional value in joint analysis of well-log data, production data, 3D and 4D seismic data, as well as 3D and 4D geomechanical models derives from the additional insight that results when either inconsistencies between the different data types occur, or when observations and predictions do not match. This enables to challenge (often unstated) assumptions in the model building, and allows model updating based on tangible and visible evidence from seismic data, drilling related and well log data, or production data.

2. Model building and Calibration

2.1. Deepwater turbidite field

The reservoir consists of deepwater turbidite sandstones (see Figure 1). Lateral extent of the oil-bearing sediments is approximately 15km. The update termination of the reservoir is given by several sealing faults. Downdip, the reservoir is connected to an aquifer. There are two main reservoirs, named the upper and lower reservoir. Each reservoir is produced separately, and wells are completed either in the upper or the lower reservoir. The updip well in Figure 1 is the discovery well and all encountered sands are fully oil saturated. The downdip well is a delineation well, and partially penetrates the water table.

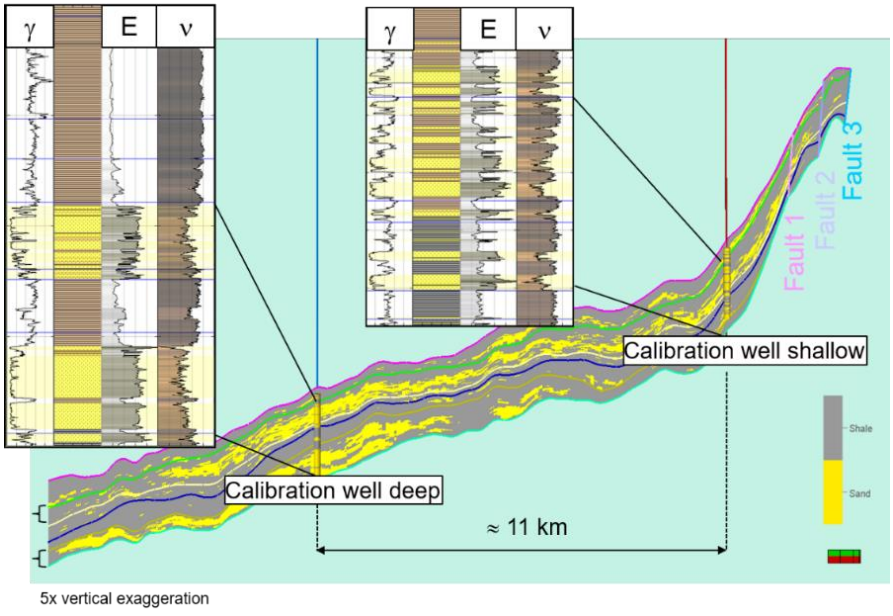

Figure 1. 2D section of a facies model together with two well-log panels.

Geomechanical logs from the discovery well (Figure 1) show the sandstones as high Youngs modulus, low Poisson ratio intervals. The lithology (sandstone or shale) is the primary variable that determines the elastic and strength parameters of the stratigraphic framework. Hence an accurate description of the facies distribution is an important factor in building a predictive 3D geomechanical model.

The sandstone intervals stronger than the surrounding shales. In a type location of a deepwater turbidite outcrop in Southern Spain (Figure 2a) this can be seen by the eroded shale beds and the protruding sandstone layers. The image was provided by Centre for Integrated Petroleum Research, Norway & University of Aberdeen and is used by permission. Note the close correspondence in thickness of beds and interlayering of shales and sandstones between the outcrop in Spain and the well-log from the case study. This picture also serves as a visual aid in understanding that stiff (high E) sandstones layers are also strong (high unconfined compressive strength and resistant to erosion). Laboratory tests show that there is a close correlation between stiffness and strength [1].

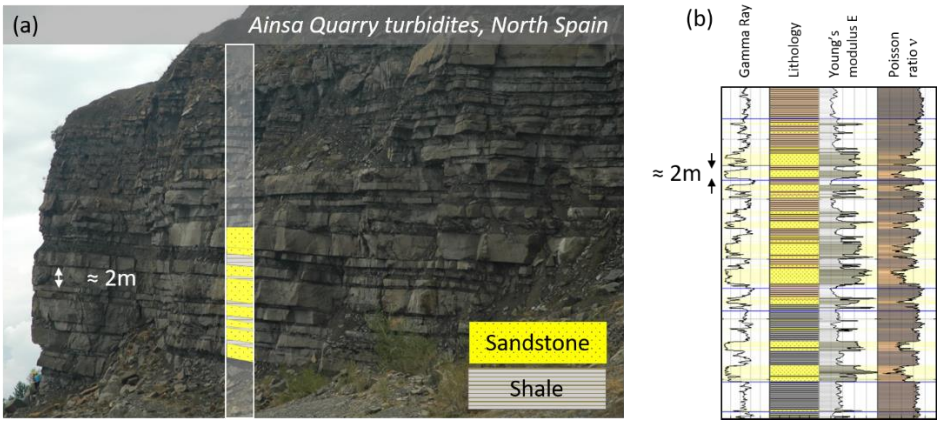

Figure 2. Mechanical stratigraphy of a deepwater turbidite in (a) outcrop and (b) well logs.

2.2. Use of seismic data in 3D property modelling

Interpreted horizons and faults from 3D seismic data interpretations are the building blocks of structural models of oil and gas reservoirs. Within the structural framework, the distribution of facies (e.g. hydrocarbon bearing sands, water bearing sands and shales) can be informed by seismic inversion techniques [2]. In this case study, the outline of the deepwater turbidite lobes was determined by results from seismic coloured inversion [3]. Figure 3(a) shows depth converted extended elastic impedance volume displayed on geological model grid. Well-log-based studies of seismic reflectivity determined the chi-angle of the lithology stack for coloured inversion to be 45^0. In so doing it can be determined that hot colours (yellow and red) in Figure 3 (a) represent

sandstones, and neutral and cold colours (grey and blue) delineate shales. The inversion results are then used as a soft property and combined with petrophysical well-logs in geostatistical property population and included into a geological facies model (Figure 3b). The geological model was then upscaled to a flow simulation model and history matched to three years of production data. Based on the geological model and the history matched flow simulation model, a 3D and 4D geomechanical flow model was built and calibrated to geomechanical models of the discovery and delineation wells.

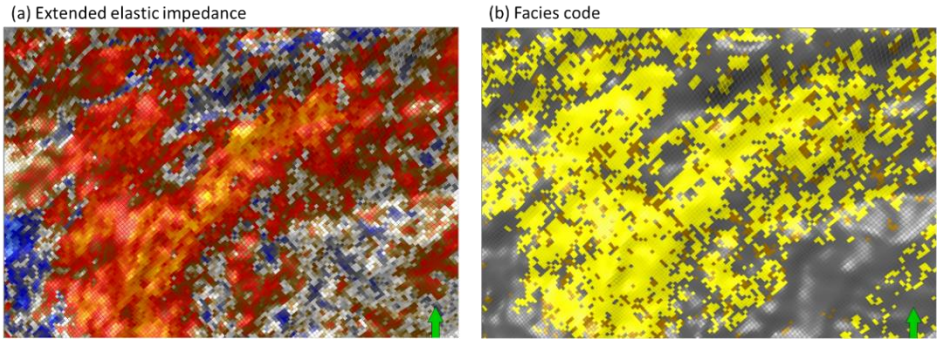

Figure 3. **(a) Lithology stack of coloured inversion mapped to reservoir grid and (b) facies model derived from co-kriging of well logs using inversion model as soft property.**

2.3. Optimized mesh for geomechanical predictions

The number of elements in a 4D and 4D computational mesh needs to be of the order of several million elements. Computational meshes with more elements would result in unacceptable run-times. Hence the average element size in the reservoir is approximately 100 m in the horizontal directions and several meters in vertical direction, and even larger in the overburden. In the near-wellbore region, stresses vary rapidly. In order to capture the known property variations in the near-wellbore and to be able to compute the near-wellbore stresses accurately, the computational mesh is refined around each wellbore (Figure 4). Similarly, the mesh in the fault zones of interest are refined.

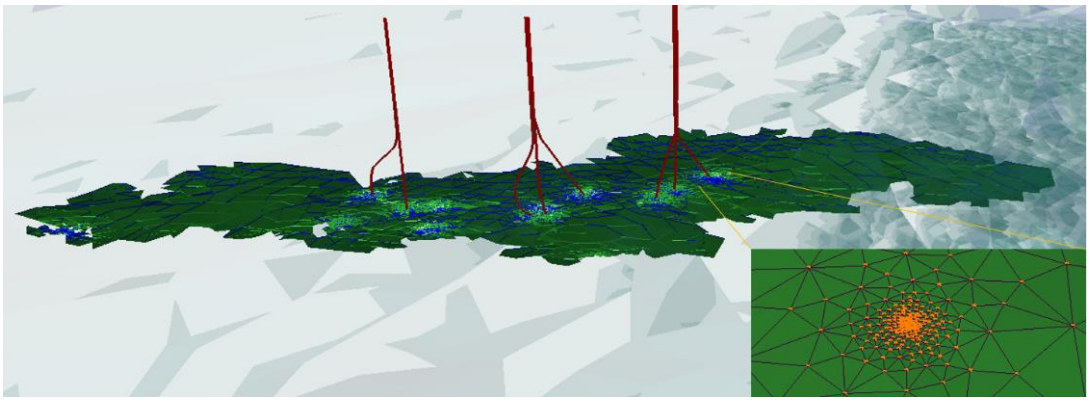

Figure 4. Mesh generation with refined meshes at wellbores and faults

2.4. Calibration of geomechanical models

Available measurements and observations which allow to infer magnitude of horizontal stresses for the case study consisted of leak-off tests at the casing shoes, caliper logs to detect deviations from circular hole shape, image logs over parts of the section, and sonic scanner logs over the reservoir interval detecting stress induced azimuthal anisotropy. The minimum horizontal stress curves of 1D geomechanical models along the two wells with a full logging suite made are made to match the inferred Shmin from the leak-off tests using the tectonic strain terms in the 1D poro-elastic equations [4],[5]. There are numerous combinations of horizontal strain terms that result in matches of the observed Shmin. Amongst these combinations, only some can explain the observed well-bore breakouts in the sandstone and the stress-induced shear-wave splitting in the sandstones from the sonic scanner measurements. In order to create wellbore breakouts in the strong sandstones, it is necessary to have a large difference in Shmin and SHmax in the sandstones (see Figure **5**). The calibrated 1D geomechanical models show SHmax in the sandstones can be larger than SV, resulting in local strike-slip stress regime (Shmin < SV < SHmax). In the shales a normal stress regime (Shmin < SHmax < SV) is observed. The same tectonic strain boundary conditions were applied for bot calibration wells shown in Figure **5**. Note the marked difference of approximately 1 MPa/km (0.85ppg) in median Shmin-gradient and SHmax-gradient between the two wells. An increase in water depth results in a decrease in stress gradient for Shim and SHmax.

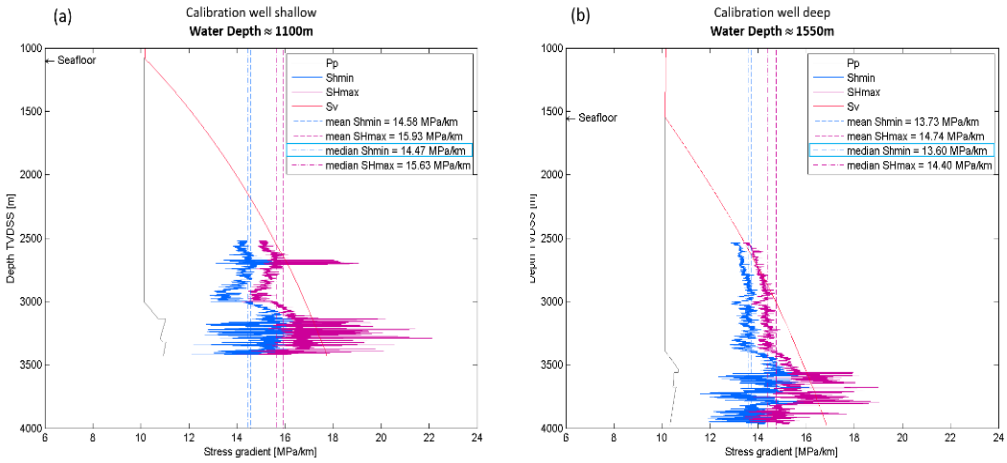

Figure 5. Stress gradient for (a) well with water depth 1100m and (b) with water depth of 1550m. Note the lower stress gradient (SV, Shmin and SHmax) in deeper water.

The tectonic strain terms from the 1D poro-elastic geomechanical models along the two calibration wells are used to derive displacement boundary conditions to be applied in the 3D finite element geomechanical model. In so doing, consistency between 1D and 3D geomechanical model is achieved (Figure 6), and no further stress calibration of the 3D finite element model is necessary. The remaining differences in calculated horizontal stresses between 1D analytical and 3D finite element geomechanical models are due to resolution of the property models.

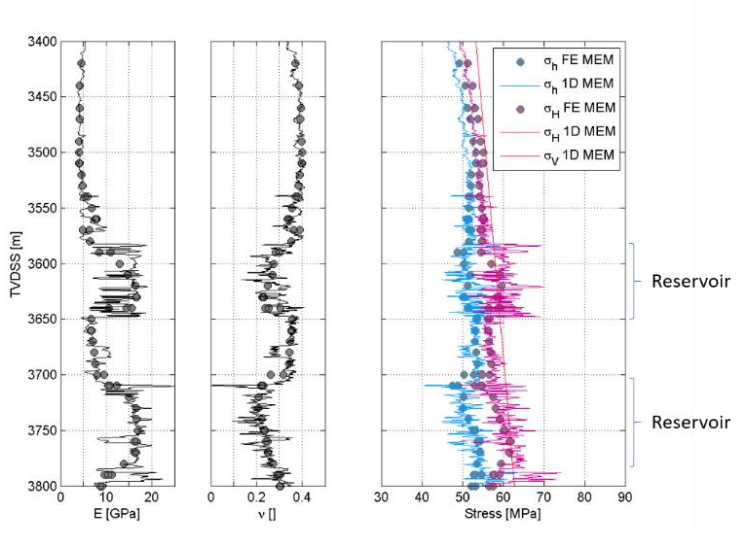

Figure 6. Calibration of 3D geomechanical model to 1D geomechanical model.

3. Applications of Geomechanical Model

3.1. Application of 3D geomechanical model to wellbore stability analysis

Wellbore stability analysis is probably the most widespread use of geomechanical studies. It is well understood that pore pressure and fracture gradient (or minimum principal stress) are independent of borehole inclination and azimuth, but that failure initiation pressure and collapse pressure (i.e. the mud pressure at which the wellbore wall is no longer sufficiently supported, and the wellbore wall starts to exhibit shear-failure and finally collapses) are not [6]. During drilling of one of the first inclined wells at the field, a stuck pipe event occurred, and the bottom-hole assembly was lost in hole (Figure 7). Geomechanical analysis showed that an elevated mudweight compared to a nearby vertical exploration well would reduce the risk of breakouts (in turn increasing the amount of solids in the hole) or wellbore collapse (as one possible cause of the stuck pipe event). Careful mud-pressure management and hole cleaning procedures enabled drilling of the sidetrack. The mudweight was thereby elevated in accordance with the mudweight prediction from the 3D geomechanical model. Figure 7(a) shows the mudweight window calculated from 3D geomechanical model for inclined trajectory. Figure 7 (b) and (c) show stereo-nets to investigate required mudweight to prevent shear failure in the wellbore wall as a function of well inclination and azimuth for depths of 3000m and 3170m TVDSS, respectively. The well and its sidetrack were drilled with an inclination of 70^0 at an azimuth of 285^0 when approaching the reservoir. Note the required increase in mudweight compared to a vertical well (Az=0^0, Inc=0^0). Finally, Figure 7(d) shows the severed drill string as a result of the stuck pipe event, caused by a combination of inefficient hole cleaning and low mudweight.

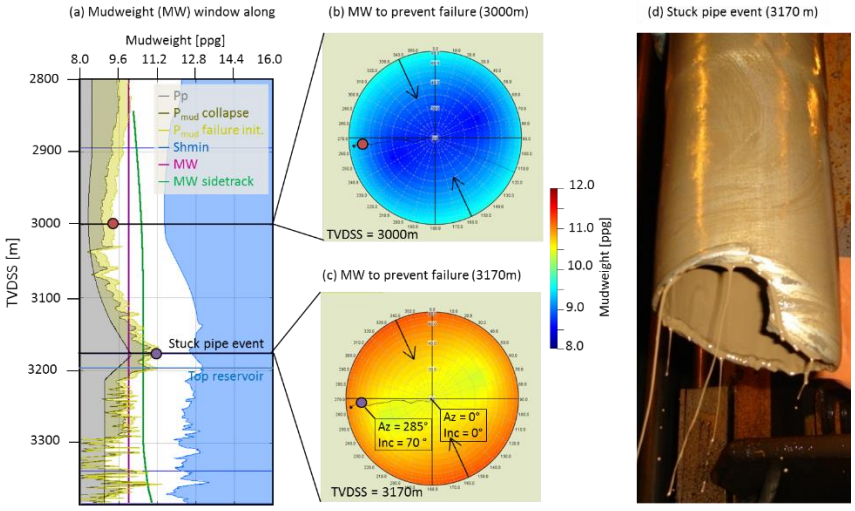

Figure7. (a) Mudweight window for inclined well, (b) and (c) stereonet plot of collapse mudweight and (d) severed drilling pipe from stuck pipe event

3.2. Fracture gradient estimation and hydraulic stimulation

The intent of hydraulic stimulation is to create a fracture penetrating through a near-wellbore damage zone that may be created during drilling and cementing of the well, hereby connecting the well to the undamaged reservoir. In stacked reservoirs, one unintended consequence of this operation can be that vertically separated reservoir zones get connected during hydraulic stimulation. This is to be avoided. To better understand the risk of out-of-zone growth of hydraulic fractures we investigated Shmin (= minimum principal stress in this field) at each completion, as well as in the caprock above each completion [7]. We take Shmin as a lower bound for fracture gradient (more precisely Shmin/TVDSS) or fracture propagation pressure. Figure 8 (a) and (b) show the results of this analysis in map view for the reservoir and the caprock respectively. In the reservoir, dots are drawn at each completion and colourcoded by the magnitude of Shmin-gradient. In the caprock the minimum fracture gradient in a 50ft interval along the well in the caprock is plotted. It becomes immediately clear that the fracture gradient in the caprock is higher than in the reservoir (darker dots in Figure 8b than in Figure 8a). Hydraulically stimulated fractures are therefore likely to stay contained within the reservoir. Note also the trend in each figure of decreasing fracture gradient from top right towards bottom left. This trend corresponds also to an increase in water depth as can be noted by the contour lines of seafloor depth in the images. Hence there is a trend of lower fracture gradient with increasing water depth. The effect of reduced fracture gradient with increased water depth can be further analysed in Figure 8(c). Analysis of the figure demonstrates that the fracture gradient is reduced by approximately 0.34 ppg for an increase in water depth per 100m (4000 Pa/m). The figure also shows that the difference in fracture gradient for the reservoir and the caprock at the same x- and y-location is on average 1ppg (1200 Pa/m).

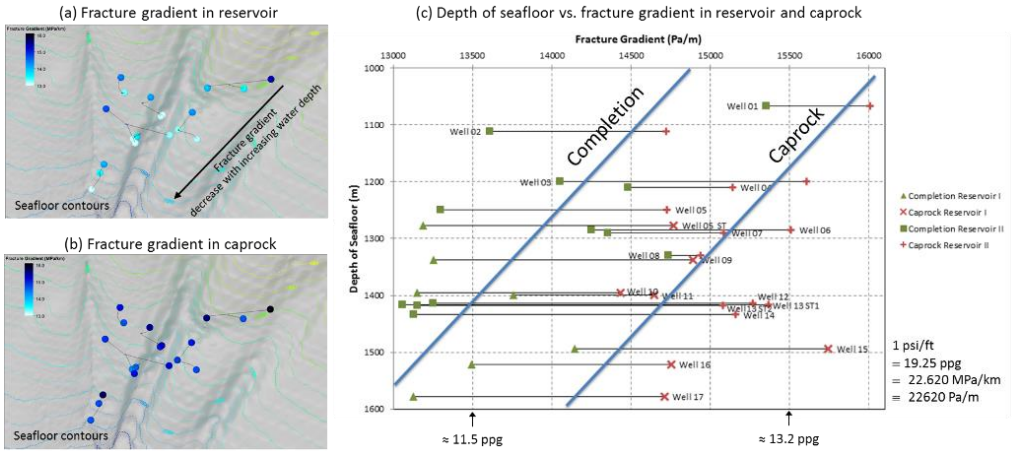

Figure 8. (a) Shmin gradient on reservoir and (b) in caprock. (c) Data from (a) and (b) summarized in a crossplot of fracture gradient as a function of water depth.

3.3. Evaluating Risk of Fault Reactivation

The reservoir terminates at an up-dip fault. A typical production scenario is to use pressure support under a voidage replacement scheme. More aggressive injection scenario can be envisaged. Such scenarios carry an increased risk of fault reactivation. In order to evaluate this risk, we compute the maximum allowable pressure increase above initial reservoir pressure along a key fault (Figure Figure 9). The fault was modelled with zero cohesion and under a range of different friction coefficients [8]. The calibration of fault mechanical properties is a field of active research and much debate. Since no direct calibration data was available for this study, we use a scenario modelling approach. As a base case we apply the generally accepted value for friction coefficients for faults of μ=0.6 [9]. Further scenarios for a weak fault (μ =0.5) and a very weak fault (μ =0.4) are tested. The distance to failure under each scenario is evaluated using the method outlined in [10].

The investigation demonstrates that the caprock forms a strong seal. Even for the scenario of the weakest fault (Figure Figure 99a), the reservoir pressure can be increased by approx. 12MPa (1750psi) above initial reservoir pressure before mechanical seal breach of along the fault occurs. Note that localized fault slip in the reservoir may occur before the entire fault plane is reactivated. One way of monitoring this mechanism would be to install permanent micro-seismic sensors in a well close to the fault. In so doing an "early warning system" for seal breach could be established.

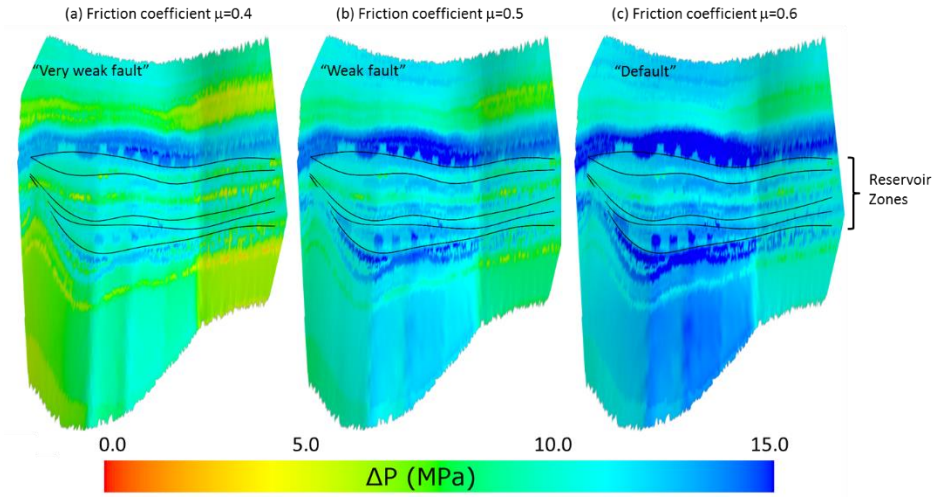

Figure 9. Pressure increase DP above initial reservoir pressure to initiate fault slip

4. Conclusions

Building a consistent integrated Earth model and taking it to 3D and 4D geomechanical flow simulation is a considerable effort. This effort may not always be justified when having only one geomechanical application in mind. However, when applying the same model to investigate several different field

development issues this effort is easily justified. This becomes apparent when summarizing some of the uses of 3D and 4D geomechanical flow models in field development planning:

- Drilling: What is the optimum mudweight window and drilling trajectory? Does the mudweight window change during reservoir production?
- Dynamic reservoir simulation and field development planning: Is there a risk of out-of-zone injection during hydraulic stimulation? Does pressure support pose a risk of fault reactivation and seal-breach? Does reservoir compaction affect fluid flow in a positive way by compaction drive or in a negative way by permeability decrease?
- Wellbore and completion integrity: Is there a risk of wellbore collapse by shear failure, compaction failure or extensional failure during production? What is the maximum allowable drawdown before onset of sanding, and what are the sand management options?

3D and 4D geomechanical models integrate data from numerous different disciplines. A welcome side effect of going through these steps is that scientists and engineers from various disciplines are forced to collaborate and communicate. Often this challenges implicit assumptions and allows a fresh look at data and their interpretations. In turn, this results in a better understanding of the behaviour of the studied field during production. Better understanding, in turn, allows informed field management decisions, safer field operations and a reduction in cost of production.

5. References

[1] Plumb, R.A., 1994, Influence of composition and texture on the failure properties of clastic rocks, Rock Mechanics in Petroleum Engineering (EUROCK '94), 29-31 August 1994, Delft, Netherlands, SPE/ISRM 28022-MS

[2] Herwanger, J.H., and Koutsabeloulis, N., 2011, Seismic Geomechanics: How to build and calibrate geomechanical models using 3D and 4D seismic data, EAGE publications, ISBN number 978-90-73834-10-1

[3] Mohamed, F.R., Rasmussen, A., Wendt, A.S., and Murineddu, A., 2008, High resolution 3D Mechanical Earth Model using seismic neural net modeling - Integrating geological, petrophysical and geophysical data, 70th EAGE Conference and Exhibition, Rome, Italy, 9-12 June, P348

[4] Thiercelin, M.J., and Plumb, R.A., 1994, Core-based prediction of lithologic stress contrasts in East Texas formations, SPE Formation Evaluation, 251-258, SPE 21847

[5] Blanton, T.L., and Olson, J.E., 1999, Stress magnitudes from logs: Effects of tectonic strains

and temperature, SPE Reservoir Eval. & Eng., 2 (1), 62-68

[6] Zoback, M.D., 2007, Reservoir Geomechanics, Cambridge University Press, Cambridge

[7] Herwanger, J.V., Bottrill, A., and Popov, P., 2016, One 4D geomechanical model and its many applications, 78th EAGE Conference and Exhibition, Vienna, 31. May 2016, DOI: 10.3997/2214-4609.201601368

[8] Wiprut, D., and Zoback, M. [2000] Fault reactivation and fluid flow along a previously dormant normal fault in the North Sea. Geology, 28, 595-598

[9] Byerlee, J. [1978] Friction of rocks, Pageoph, 116(4-5), 615-626

[10] Mildren, S.D., Hillis, R.R., and Kaldi, J. [2002] Calibrating predictions of fault seal reactivation in the Timor Sea. APPEA Journal, 42, 187-202